This full-text paper was peer-reviewed at the direction of IEEE Instrumentation and Measurement Society prior to the acceptance and publication

Validating Inertia Assessment Metrics in Distribution Systems with High RES Penetration

Guglielmo Frigo
Federal Institute of Metrology
METAS
Bern-Wabern, Switzerland
guglielmo.frigo@metas.ch

Virginia Negri, Alessandro Mingotti, Roberto Tinarelli, Lorenzo Peretto
Department of Electrical, Electronic and Information Engineering "Guglielmo Marconi"
Alma Mater Studiorum - University of Bologna
Bologna, 40136, Italy
virginia.negri2, alessandro.mingotti2, roberto.tinarelli3, lorenzo.peretto@unibo.it

Johan Rens, Theresa Joubert
School of Electrical, Electronic, and Computor Engineering
North-West University,
Potchefstroom, South Africa
johan.rens@nwu.ac.za
jouberttheresa15@gmail.com,

2024 IEEE 14th International Workshop on Applied Measurements for Power Systems (AMPS) | 979-8-3503-7531-2/24/$31.00 ©2024 IEEE | DOI: 10.1109/AMPS62611.2024.10706692

***Abstract*— The role of inertia in distribution networks is rapidly increasing. Many researchers are focused on ways to estimate, measure, and control inertia, as it has become a crucial parameter that provides valuable information for network management. However, the distribution network is not as stable and has many more nodes compared to the transmission network. Additionally, the distribution network is populated with various renewable energy sources. While this brings several advantages, such as reducing fossil fuel-based energy production and adjusting voltage in remote nodes of the network, it also significantly impacts the network's inertia due to the removal of rotating electrical assets in favor of renewable sources. To address this issue, the paper tests a new inertia metric on a section of a real network with significant presence of renewables. This metric, calculated using frequency and power measurements, demonstrates a strong capability to reflect the current state of inertia in the network. The paper concludes with a description of the network under consideration, the instrumentation used, and a brief uncertainty analysis.**

Keywords*— Inertia, ROCOF, frequency, metrics, accuracy, renewables, uncertainty, distribution network

I. INTRODUCTION

Power system management requires knowledge of system frequency and its rate of change. Tracking the Rate of Change of Frequency (ROCOF) helps power system operators maintain system dynamic stability. When the balance between generation and load is disturbed, the frequency can deviate from the nominal values of 50 Hz or 60 Hz. The rate at which frequency changes from one value to another is influenced by the availability of inertia in the interconnected power system. The working principles of an AC power system rely on the inertia within large synchronous generators, as it supports system dynamic stability by damping sudden changes in frequency. If sufficient inertia is available in a power system, a low ROCOF can be maintained, allowing for a safe and predictable transition between different states of power system operation.

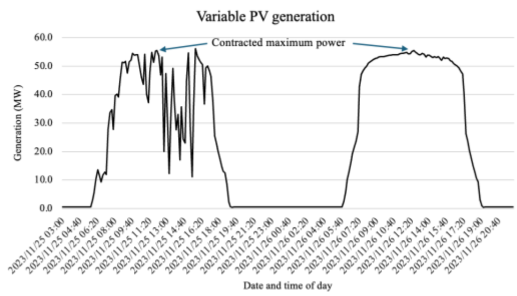

Fig. 1. A real-world example on PV production variability

Renewable power plants (RPPs) that convert energy from wind and photovoltaic (PV) sources inject power into the AC power system mostly through solid-state interfaces but do not store inertia in a mechanical system [1]. Maximum power production from these sources can be highly variable due to sudden and unpredictable changes in solar irradiation or wind speed. An example of the daily production at a grid-connected PV plant is shown in Fig. 1. In the graph it can be appreciated how power production suddenly changes up to 80 %.

An RPP typically does not participate in energy dispatch strategies and generates as much power as possible all the time. If a large portion of total power generation comes from RPPs, such sudden changes in generation can constrain effective frequency control measures. In a traditional power system, a sudden mismatch between generation and load typically results from a change in loading, not due to a change in generation as is the case with an RPP.

While it is possible to emulate inertia from solid-state generators, the extent to which this can be done is limited and requires longer reaction times compared to synchronous generators [2]. As engineering and technical considerations are not the only factors affecting the mix of generation

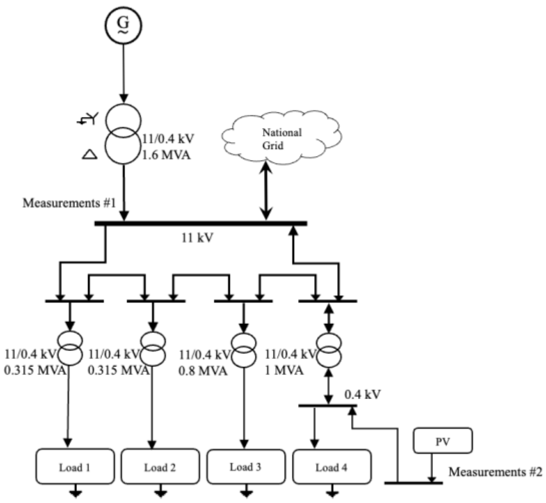

Fig. 2. Schematic of the distribution network described and used in this work

sources in modern power systems—political and environmental factors also play a role—RPPs are often preferred over traditional thermal solutions. Consequently, the availability of inertia decreases as renewable energy generation increases.

From the above discussion, it is evident that accurate knowledge of the available inertia in a power system is crucial for planning strategies to mitigate system frequency variations [3].

This paper evaluates practical solutions for tracking inertia in a distribution system with integrated renewable energy sources. In particular, the focus is on the adoption of a specific metric to quantify inertia and assess the status of the grid. Recent literature has proposed different metrics and methods to evaluate inertia variations [4]. In the vast majority, a numerical routine provides an evaluation of the overall system stability, based on a set of distributed synchronized measurements [5]. In this paper, instead, we focus on a local approach [6]. Based on the measurements collected in a single node of the network, we attempt to detect and identify inertia variations. Differently from the systemic methods, such an approach allows for evaluating the response of each node as a separate agent and potentially detect inconsistencies between the expected and the actual behavior of the closest generating unit.

The remainder of the paper is structured as follows. Section II reviews the basic principles of inertia and highlights the goal of the paper. The distribution network considered in the case study is described in Section III. In Section IV, instead, the experimental activity and the main results are presented. Finally, Section V draws the conclusion.

II. Principles of Inertia

This section introduces some basic principles about inertia, recent developments, and the main goal of this study.

A. Inertia

Mechanical inertia within power systems serves to mitigate imbalances between generation and load demand so limiting frequency fluctuations. Monitoring instantaneous power system frequency offers insight into the equilibrium between generation and loading in an AC power system. Inertia plays a critical role in moderating the ROCOF, ensuring sufficient stability for dynamic operations. For instance, the South African grid code [7], akin to other international standards, advocates for a ROCOF of less than 0.5 Hz/s for optimal performance [2].

To quantify available inertia, an inertia constant is defined, drawing from the mass and power rating of the mechanical generation system and the angular velocity of the rotating mass. The widely used swing equation expresses the power equilibrium (or imbalance) during abrupt disparities between generation and loading.

Considering a scenario where there is a sudden reduction in loading, the swing equation is represented by:

$$2H\frac{df(t)}{dt} = \Delta P_m(t) - \Delta P_e(t) = \Delta P(t), \quad (1)$$

where:
H: Synchronous generator inertia constant, in seconds (s).
f: frequency at synchronous generator terminals, in Hz.
$\Delta P_m(t)$: Change in mechanical power, W.
$\Delta P_e(t)$: Change in electrical power, W.

During an electrical power transient, being a relatively rapid occurrence in an electrical system, the mechanical system, and specifically the mechanical power, remains relatively stable throughout the duration of such rapid electrical transient, leading to the simplifying hypothesis that $\Delta P_m(t) \approx 0$. Therefore, starting from (1), the inertia constant H at $t = t_0$ can be well approximated by:

$$H \simeq \left| \frac{-[P_e(t_0^+) - P_e(t_0^-)]}{2\left[\frac{f(t_0^+) - f(t_0^-)}{t_0^+ - t_0^-}\right]} \right|, \quad (2)$$

with t_0^- and t_0^+ indicating the time instants before and after the power transient. The frequency derivative is approximated as the finite-difference incremental ratio of the frequency values in the two considered time instants. In (2), the absolute value is intended to guarantee that the inertia constant is a positive quantity. Nevertheless, it is also worth noticing that in practice power and frequency variations are typically characterized by opposite signs. A reduction in the power demand (i.e., $\Delta P_e < 0$) corresponds to a system frequency increase, and viceversa.

B. The goal of this paper

Considering the above, this paper aims to experimentally validate inertia metrics, proposed by the authors, in a distribution network where a significant penetration of RES exists. To this purpose, power, frequency, and ROCOF measures obtained from a South African distribution network were used. The metrics are then validated by extensive analysis of the results. Opportunities on the pragmatic application of these metrics are then discussed.

III. Description of the Distribution System

The following subsections present the distribution network considered in this study and the instrumentation used to collect the field data used in the analysis of the inertia metrics.

A. Distribution network configuration and states

A simple schematic of the distribution network that serves a Southern African (SA) university campus is shown in Fig. 2. The 11 kV 50 Hz ring-feed network serves end-users at 400 V. Under normal conditions, this distribution network is grid connected where generation sources are from a mix of turbine-generators and various renewable sources such as wind, sun and water.

Within this local network, a 50 kVA grid-connected rooftop photovoltaic (PV) system reduce the energy flow from the national grid. The national grid is disconnected several times each day. A 400 V 800 kVA diesel generator then supplies the majority of the energy demand. The PV inverters will shut down when the national grid disconnects, but will synchronize to the diesel generator that starts within a few seconds when the local grid is islanded.

The impact of the embedded PV system, quantified as the "penetration level of PV" [8], can be expressed by the ratio:

$$Penetration = \frac{PV\ Power}{Load\ Demand} \quad (3)$$

In the considered distribution system, the penetration level stands at approximately 26 %, with a load demand of nearly 200 kVA, and PV barely exceeding 50 kVA. This configuration is a controlled experimental setup as all contingencies can be reliably correlated to the field measurements.

In South Africa, national frequency control relies on scheduled disconnections of various network segments to match loading with available generation. These disconnections occur differently in different regions, in approximately 2-hour intervals. During such event the campus network is an islanded distribution network.

Upon loss of connection to the national grid, the entire distribution network experiences a power outage. Within a minute, the generator supplies energy, followed by synchronization of PV inverters within a few seconds. The amount of PV energy available depends on the daily solar irradiation. When the national grid is restored, the diesel generator synchronizes with the grid before disconnecting, ensuring an uninterrupted transition from diesel generation to the national grid. The PV inverters remain connected during this stage.

The sequence of events described above introduces significant variations in available inertia, facilitating comprehensive and comparative evaluations of stability quantification based on inertia availability in the distribution grid. To validate the mathematical implementation of the methodology for deriving inertia and subsequent assessment of frequency stability, this network underwent detailed modeling and simulation using DIgSILENT™.

Overall, four states of system inertia in the distribution system are considered in this paper:

- Only the national grid: The national grid is the only energy source, but with variable levels of traditional inertia and without any local embedded generation.
- Daytime with PV: The national grid is complemented by PV during daytime.
- Islanded state: Only diesel generation during night-time.
- Daytime with diesel and PV: Diesel generation is supported by PV generation during daytime.

All network states were known and correlated with the field data used to study the tracking of system inertia.

B. Instrumentation and field data

At every measurement point, the voltage and the current were measured with a Vectograph 3, that is a power quality instrument certified as compliant to the measurement requirements of IEC 61000-4-30, Class A, edition 3 [10]. The sampling rate of 500,000 Sa/s collected the 10/12 cycle blocks of waveform data. The manufacturer specify an accuracy of 0.1 % in the measurement range 10 % to 100 % of the rated quantity.

The reporting rate of the device is 200 ms. Computed quantities of interest were frequency, ROCOF, and active power, measured simultaneously at different points with a time-stamping uncertainty better than ±100 ns.

IV. EXPERIMENTAL ACTIVITY

This section discusses the data collection, inertia metrics, and results obtained.

A. Data collection

Synchronous measurements were obtained where the inverters connect to the local 400 V bus and at the 400 V bus where the generation injects via a 11/04 kV transformer into the 11 kV ring, as shown in Fig. 2. The national grid connects at 11 kV.

B. Inertia metrics

Robust solutions to the quantification of inertia remains a topic of interest at transmission and distribution system operators [11]. In traditional power systems, this information could be derived from the inertia constants of different synchronous machines and other parameters from the network topology.

When a significant portion of generation is obtained from solid-state generators, knowledge on inertia becomes more complicated [12]. On one hand, the power output of renewable generation sources are not necessarily correlated to the system frequency or system operating point [13]. On the other hand, the concept of inertia constant may lose its significance if the response of a generating unit during a load change does not rely on a physical property such as mass, but is now controlled by power electronics [14]. Based on these considerations, it is preferred to study the response of the power system by the variations of inertia as a function of time.

Such an analysis could provide useful information about the stability of the power system and could be used to select the most suitable and effective control action to prevent service disruptions or (in the worst case) system contingencies [15].

Let's assume to measure, at each node of interest, the system frequency f and the active power P at a fixed reporting rate. In the presence of a sudden change in the operating conditions, it is possible to evaluate a stability index I_H related to the inertia constant H based on the time derivatives of f and P:

$$I_H(t_1) = \frac{\Delta P}{2 \cdot \Delta\left(\frac{df}{dt}\right)} = \frac{P(t_1) - P(t_0)}{2 \cdot \left(R_f(t_1) - R_f(t_0)\right)} \quad (4)$$

where t_1 and t_0 are two consecutive reporting instants, and R_f denotes the ROCOF. It is worth noting that I_H does not account for the system inertia constant but allows for detecting anomalous behaviors in a rapid and immediate manner. Its variation range depends on many factors: e.g., the power flows in the node of interest, the method to measure the frequency and its derivative, and noise level. It is thus necessary to perform an accurate evaluation of its statistical distribution in normal operating conditions before configuring any anomaly detection rule.

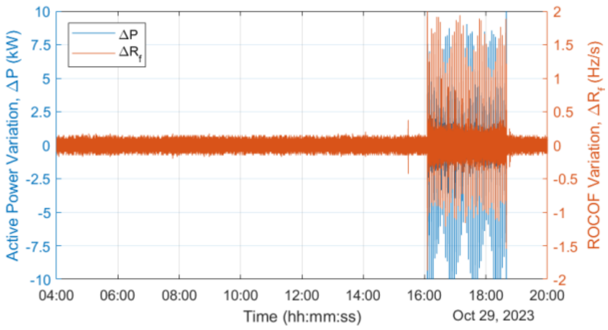

(a) Measurement point #1

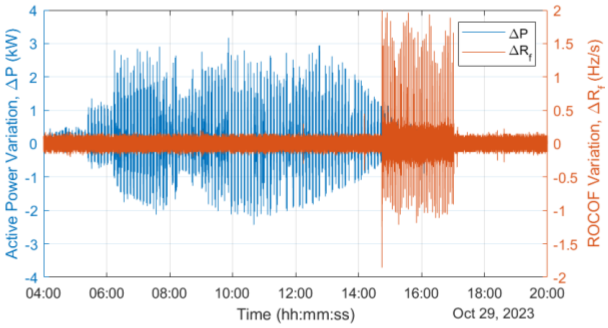

(b) Measurement point #2

Fig. 3. Variations of active power (blue) and ROCOF (red) as measured at measurement point #1 and #2 in (a) and (b), respectively.

(a) (b)

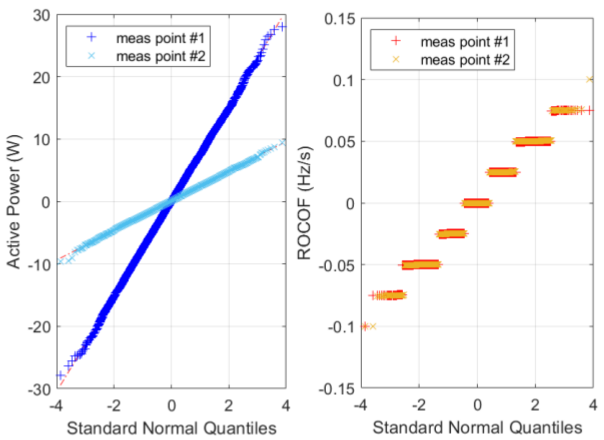

Fig. 4. Quantile-quantile plots for active power and ROCOF in normal operating conditions in (a) and (b), respectively.

C. Results

Till now, the stability index (4) has been tested only in numerical simulations. To validate its feasibility and reliability in real-world scenarios, the index is tested on the dataset presented in Section IV.A and relative to the distribution network introduced in Section III. For the sake of brevity, the analysis will focus on a restricted set of measurements, but similar results could be obtained on larger datasets.

For this analysis, the considered measurements were performed on October 29th, 2023, at the measurement point #1 and #2, as identified in Fig. 2. The first one, close to the interconnection with the national grid, is representative of the overall system state. The second one, instead, is directly affected by the functioning of the PV power plant, i.e. it reflects the effects of the distortions introduced by power converter circuitry as well as the instability due to the inherent solar irradiance volatility.

During daylight period, the distribution network is relying on the PV power plant. In the absence of sufficient solar irradiance or during night period, the diesel generator and the connection with the national grid guarantees the continuity of service. This behavior is confirmed by the time evolution of the variations in active power and ROCOF in Fig. 3. At the measurement point #1, both quantities remain constant (affected only by measurement noise) until 15:00, when the diesel generator is started. Conversely, at the measurement point #2, the power variations reflect the solar irradiance profile. Also in this case, around 15:00, disturbances are noted.

It is interesting to observe how the ROCOF remained constant (affected only by measurement noise) while the PV power plant is active, whereas it exhibits fast switching spikes as soon as the diesel generation units are started.

First, the measurement noise at both measurement points and for both quantities must be characterized. To this end, it a time span of two hours where no significant actions took place was considered: from 04:00 to 06:00 for measurement point #1, and from 18:00 to 20:00 for measurement point #2. In this regard, Fig. 4 presents the quantile-quantile plots of the power and ROCOF variations for the two measurement points.

The power measurements have a normal distribution between ± 30 and ± 10 W at measurement point #1 and #2, respectively. This confirms the assumption that the measurement noise is uncorrelated as it is normally distributed. Conversely, the ROCOF measurements are mostly affected by quantization noise, as the instrument has a finite resolution of 25 mHz/s.

Based on the distributions in Fig. 4, specific thresholds can be set on active power and ROCOF. It is needed to determine whether the variable of interest is varying and diverging from its nominal value, or if it is only the inherent uncertainty contributed by the measurement procedure. In this case, any active power variation lower than ± 30 W or ROCOF variation lower than ± 0.1 Hz/s are neglected for the computation of the system stability index I_H.

In the dataset under investigation, power and ROCOF variations were computed every 200 ms. However, such a restricted time-horizon may prove to be not so significant in terms of system stability assessment. For this reason, power and ROCOF variations are first processed via a moving average window with a duration of 10 s (i.e., corresponding to 50 consecutive measurement periods). This has a twofold advantage. It reduces the effect of additive uncorrelated noise (in particular, in the power measurements) and it smooths out the spikes due to switching events (in particular, in the ROCOF measurements). Secondly, similar to a Type-A uncertainty or confidence interval, when computed as the 95th percentile of the 50 values included in the moving average window, it can be associated to each average value.

In this regard, Fig. 5(a) presents the confidence interval associated with the ROCOF average values in both datasets. It is interesting to observe how this interval is consistent with the distribution shown in Fig. 4(b), apart from the time interval between 16:00 and 18:00, when the diesel generator kick in.

Based on these results, the stability index associated to measurement point #1 and #2 can be computed. For this analysis, only the intervals where both active power and ROCOF show variations whose confidence intervals exceed the expected noise level, are considered. The results are presented in Fig. 5(b). In terms of the PV power plant, the

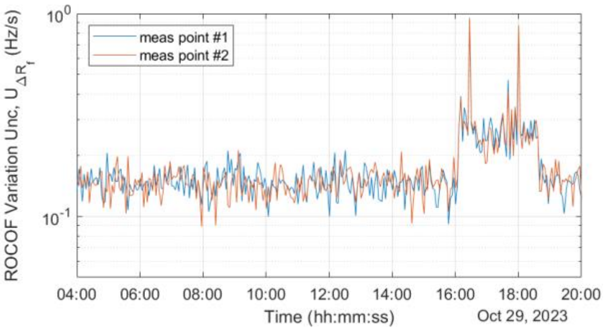

(a)

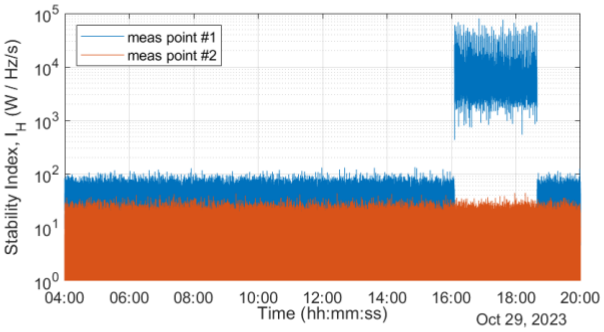

(b)

Fig. 5. In (a), confidence intervals associated to ROCOF variations in both measurement points. In (b), stability indices computed as per (4). Blue and red lines refer to measurement point #1 and #2, respectively.

system appears to be in a stable condition: the active power variations (due to the corresponding solar irradiance variations) do not impact the signal frequency and ROCOF, At the instance when ROCOF becomes irregular (around 16:00), the power output is nearly zero and why the stability index remains unaffected.

Conversely, at measurement point #1, the system shows a sudden change in correspondence of the diesel generators' start. In this case, the variation in active power and in ROCOF are significant and uncorrelated. Consequently, the stability index significantly increases as indication to the system operator and system engineers that some anomaly has occurred.

V. Conclusion

This study emphasized the growing importance of tracking inertia in distribution networks and the challenges posed by the integration of renewable energy sources. The instability and complexity of distribution networks, coupled with the shift from traditional rotating electrical assets to renewables, necessitate new approaches to estimate, track, and control inertia. The distribution network considered was a perfect testbench to assess the implementation of a new inertia metric under known network conditions. During the testing, many different ROCOF events were recorded, to allow reliable assessment of the efficacy of the proposed new metric under real-life conditions. Future studies will be dedicated to the validation of the proposed work in different real and simulated scenarios. This work provides a foundation for future research to develop practical applications aimed at enhancing the stability and reliability of distribution networks in the evolving energy landscape.

References

[1] N. Hatziargyriou, J. Milanovic, C. Rahmann, V. Ajjarapu, C. Canizares, I. Erlich, D. Hill, I. Hiskens, I. Kamwa, B. Pal, P. Pourbeik, J. Sanchez-Gasca, A. Stankovic and T. Van Cutsem, "Definition and Classification of Power System Stability – Revisited & Extended," *IEEE TRANSACTIONS ON POWER SYSTEMS,* vol. 36, no. 4, pp. 3271-3281, 2021.

[2] P. Denholm, T. Mai, R. W. Kenyon, B. Kroposki and M. O'Malley, "Inertia and the power Grid: A guide without the spin," NREL, Colorado, 2020.

[3] Costa, F., Mingotti, A., Peretto, L., & Tinarelli, R. (2022). A simple approach to quantify accuracy of power systems inertia. Paper presented at the 2022 12th IEEE International Workshop on Applied Measurements for Power Systems, AMPS 2022 - Proceedings, doi:10.1109/AMPS55790.2022.9978840.

[4] B. Tan, J. Zhao, M. Netto, V. Krishnan, V. Terzija, Y. Zhang, Power system inertia estimation: Review of methods and the impacts of converter-interfaced generations, in: International Journal of Electrical Power & Energy Systems, vol. 134, art. no. 107362, Jan. 2022.

[5] F. Gonzalez-Longatt, J. M. Roldan-Fernandez, H. R. Chamorro, S. Arnaltes, J. L. Rodriguez-Amenedo, Investigation of Inertia Response and Rate of Change of Frequency in Low Rotational Inertial Scenario of Synchronous Dominated System, in: Electronics, vol. 10, art. no. 2288, Sept. 2021.

[6] F. Costa, L. Peretto and G. Frigo, "PMU-Based Estimation of Inertia Variation: Proposed Metric and Feasibility Analysis," 2023 IEEE International Instrumentation and Measurement Technology Conference (I2MTC), Kuala Lumpur, Malaysia, 2023, pp. 1-6.

[7] Grid connection code for renewable power plants (rpps) connected to the electricity transmission system (ts) or the distribution system (ds) in south africa, 2022

[8] C. K. CHang, "Data-driven Estimation of the Power Grid Inertia with Increased Data-driven Estimation of the Power Grid Inertia with Increased Levels of Renewable Generation Resources Levels of Renewable Generation Resources," Syracuse University, Syracuse University, 2022.

[9] www.CTLAB.com. Accessed on 01/05/2024.

[10] IEC 61000-4-30:2015+AMD1:2021, Electromagnetic compatibility (EMC) - Part 4-30: Testing and measurement techniques - Power quality measurement methods.

[11] R ENTSO-E, Project Inertia – Phase II: Updated Frequency Stability Analysis in Long Term Scenarios, Relevant Solutions and Mitigation Measures, Nov. 2023.

[12] M. Paolone et al., Fundamentals of power systems modelling in the presence of converter-interfaced generation, in: Electric Power Systems Research, vol. 189, art. no. 106811, Dec. 2020.

[13] H. Yin et al., Field Measurement and Analysis of Frequency and RoCoF for Low-Inertia Power Systems, in: IEEE Transactions on Industrial Electronics, vol. 71, no. 7, pp. 7996-8006, July 2024.

[14] M. Yu et al., Instantaneous penetration level limits of non-synchronous devices in the British power system, in: IET Renewable Power Generation, vol. 11, no. 8, pp. 1211-1217, Jan. 2017.

[15] ENTSO-E, Frequency Measurement Requirements and Usage, Jan. 2018. Online [accessed 13 Apr. 24] https://docstore.entsoe.eu/Documents/SOC%20documents/Regional_Groups_Continental_Europe/2018/TF_Freq_Meas_v7.pdf.